Interactions between Al–1 wt% Si thin film and W–Ti barrier layer

PENG-HENG CHANG, HUEI-MING CHEN
Institute of Materials Science and Engineering, National Chiao Tung University, Hsinchu, Taiwan
HUNG-YU LIU, J. G. BOHLMAN
Materials Science Laboratory, PO Box 655936, M/S 147, Texas Instruments Inc., Dallas, Texs, 75265, USA

The interaction of Al–1 wt% Si with a W–Ti barrier layer in the $Al/Ti_3W_7/SiO_2/Si$ system was studied over the temperature range of 400–500 °C for reaction times up to 300 h. The interaction was found to be diffusion-controlled, and to occur in a layer-by-layer fashion. The first reaction product is always $Al_{12}W$, which forms at the Al/Ti_3W_7 interface. With excess W in the system, Al will eventually be completely converted to $Al_{12}W$, and further interactions result in the formation of an Al_4W layer at the $Al_{12}W/Ti_3W_7$ interface. The amount of Al_4W increases at the expense of $Al_{12}W$. Ti plays a minor role in the interaction and forms a small amount of Al_3Ti precipitates in the $Al_{12}W$ matrix. Decomposition of the Ti_3W_7 pseudoalloy into W and Ti phases is not significant, and is not detected by X-ray diffraction even after annealing at 500 °C for 300 h. The kinetics of the $Al_{12}W$ formation follows a parabolic reaction law with an activation energy of 2.53 eV. The sheet resistance of the film is insensitive to compound formation as long as a continuous Al film exists in the system. The sheet resistance increases dramatically when Al is consumed to the extent that it is no longer a continuous film. The sheet resistance of the $Al_{12}W$ layer is estimated to be 570 $m\Omega\ \square^{-1}$.

1. Introduction

Aluminium films containing small amounts of Si and/or Cu have been extensively utilized as interconnects or contacts in very-large-scale integration (VLSI) [1, 2]. As the device dimensions are scaled down, the increased current density results in more stringent limitations on the interactions between Al and substrate Si. Various diffusion barrier layers have been developed to prevent interdiffusion between Al and Si [2, 3]. Yet none of the barrier layers developed so far is completely inert. Interactions between a barrier layer and its neighbouring films may occur during subsequent processing, leading to catastrophic failure. For example, Al films (with or without Si or Cu) have been shown to interact with the W–Ti layer, a commercially important interdiffusion barrier in VLSI processes [3–14]. The detailed interactions between Al and W–Ti vary with the substrate underneath and with the Ti content in the W–Ti barrier layer. For Al(2% Cu)/Ti_3W_7 deposited on an amorphous Si substrate, the interdiffusion of Al and Si across the Ti_3W_7 layer was so significant at 450 °C that TiSi, $TiSi_2$, and $(Ti_6W_4)Si_2$ silicides were formed at the Al/Ti_3W_7 interface, and two additional compounds, WSi_2 and $AlTi_3$, were also formed at temperatures higher than 500 °C [4]. Similar results were observed when Al(0.8% Si)/Ti_3W_7 layers were deposited on a polycrystalline Si substrate [5]. In this case the Ti_3W_7 is also ineffective as a diffusion barrier, resulting in the formation of TiSi, $TiSi_2$, Al_3Ti and $Al_{12}W$ compounds. The same Ti_3W_7 layer interposed between an Al film and a single crystalline Si (*c*–Si) substrate is, on the other hand, quite a stable barrier layer up to about 500 °C [6, 7]. Intermixing between Al and W at the Al/TiW interface was detected by Auger [10] and Rutherford backscattering spectrometry [7] in the Al/Ti_3W_7/*c*-Si system at higher temperatures, indicating a possible $Al_{12}W$ compound formation as in the case of Al/TiW/SiO_2/*c*-Si system [8–12]. In the latter system, the SiO_2 layer is typically formed by thermally oxidizing a single crystalline Si substrate. The dominant interaction in the Al/TiW/SiO_2/*c*-Si system is between Al and W if the Ti content of TiW is less than 30 at %. $Al_{12}W$ is always the first compound to form at the Al/TiW interface in this system [3, 8–12]. If the Al to TiW ratio is small, a further reaction would lead to the formation of Al_5W and/or Al_4W at the expense of $Al_{12}W$ [8–10].

The Ti content in a TiW layer affects its crystal structure and the subsequent interactions with the overlaying Al layer. For a Ti content of 40 at % or lower, the observed crystal structure of TiW is the body centred cubic structure of W, while the hexagonal structure of α-Ti dictates for Ti content of 80 at % or higher [13]. The dominant reaction product between Al and TiW layers is Al_3Ti for Ti-rich TiW and Al/W compounds ($Al_{12}W$, Al_5W, Al_4W) for W-rich

0022–2461 © 1994 Chapman & Hall

TiW [8–11, 14]. In W-rich Al/TiW/SiO_2/c-Si systems, titanium has been shown to out-diffuse to the top surface by Rutherford back-scattering spectrometry [3] and by secondary ion-mass spectrometry [9]; small Al_3Ti precipitates were also observed in the $Al_{12}W$ grains by transmission electron microscopy (TEM) at temperatures higher than 500° C [9]. In one report [12], Al_3Ti was also observed inside an annealed Ti_2W_8 film near the Al/TiW interface, indicating a possible penetration of Al into the TiW layer. The kinetics of the Ti out-diffusion from W-rich TiW have been examined extensively by Rutherford backscattering spectrometry and an activation energy of 2.4 eV was reported [3]. But the kinetics of the dominant interactions in the W-rich Al/TiW/SiO_2/c-Si system, namely the formation of $Al_{12}W$, Al_5W, and Al_4W, have received very little attention. One attempt has been made by the present authors to study the kinetics of $Al_{12}W$ formation using X-ray diffraction (XRD) [15]. Since the X-ray peak intensity from the $Al_{12}W$ phase is typically small, especially in the initial stage of the interaction, we used the Al (1 1 1) peak intensity variation as an indicator for the $Al_{12}W$ reaction kinetics, and an activation energy of 1.5 eV was suggested for the $Al_{12}W$ formation in the Al/TiW/SiO_2/c-Si system. This approach, however, is considered inadequate and the 1.5 eV obtained inaccurate, for the following reasons: (i) as more than one compound is formed as the result of the Al/TiW interaction, the change in the Al (1 1 1) peak intensity cannot be ascribed to the formation of $Al_{12}W$ alone; and (ii) due to process variation, the initial thickness of Al film varied from wafer to wafer, and as we used companion wafers in the X-ray study this variation was inevitable, rendering the absolute Al peak intensity unsuitable for quantitative analysis. Since the need still exists we have therefore undertaken a more reliable, quantitative study of the thin-film interactions between a W–10 wt % Ti barrier layer and an Al layer containing 1 wt % Si in an Al/TiW/SiO_2/c-Si system, depending more on transmission electron microscopy (TEM) and electrical data for the kinetics study, and only using the XRD data for qualitative support. The detailed microstructural evolution and the correlation between the electrical properties and microstructures in this system will be discussed also.

2. Experimental procedure

W–Ti films, ~ 0.3 μm thick, were deposited *in situ* in a D.C. magnetron-sputtering deposition machine from a W–10 wt % Ti (30 at %) target onto oxidized, four-inch, p-type, ⟨1 0 0⟩ Si wafers. The thickness of the thermal oxide layer was about 0.1 μm. A nominal 0.5 μm-thick Al–1 wt % Si layer was further deposited on top of the W–Ti layer in the same machine without breaking the vacuum. The wafers, one for each temperature–time condition, were annealed in hydrogen at 400, 450, or 500 °C for times varying from 1 to 300 h. The sheet resistance of each annealed wafer was measured with a four-point probe and its microstructures examined by TEM and thin-film XRD. Cross-sectional TEM specimens were prepared from the annealed wafers in the usual fashion, as reported previously [16] and examined with a JEOL 2000FX microscope operating at 160 kV. XRD was performed at room temperature on annealed samples using Huber diffractometry with a Seeman–Bohlin geometry. The sample surface was placed at a tangent to the diffraction circle. The monochromatic beam of Cu $K_{\alpha 1}$ was focused at the intersection of the circle defined by a curved quartz single crystal and the diffraction circle. The sample surface was stationary with respect to the incident X-ray, making a glancing angle of about 2.5° while the counter was swinging along the diffraction circle to collect the diffracted X-ray at appropriate 2θ angles.

3. Results and discussion

Figs 1–3 show the XRD patterns for samples annealed at 400, 450 and 500 °C, respectively. Note that the patterns were plotted in a semi-log scale in order to enhance the weaker peaks from the minute reaction products which might be present. Although experimentally the 2θ scan in each X-ray run covered from 20° to 120°, we only show the results from the angular range of 20° to 50° in these figures (for brevity, and because the data within this range are sufficient to reveal all the salient changes relevant to the thin-film interactions). The diffraction peaks in each figure were identified and the corresponding phases were labelled as marked. In Fig. 1, it is clearly seen that the 1- and 3-h patterns are practically the same, and contain only peaks from Al and W, indicating that the interaction between Al and W is minimal (if it exists at all). Evidence for some interaction is barely observable in the 30-h sample as revealed by the small peak at 28.8° in the 30-h pattern, which was ascribed to the (2 1 1)

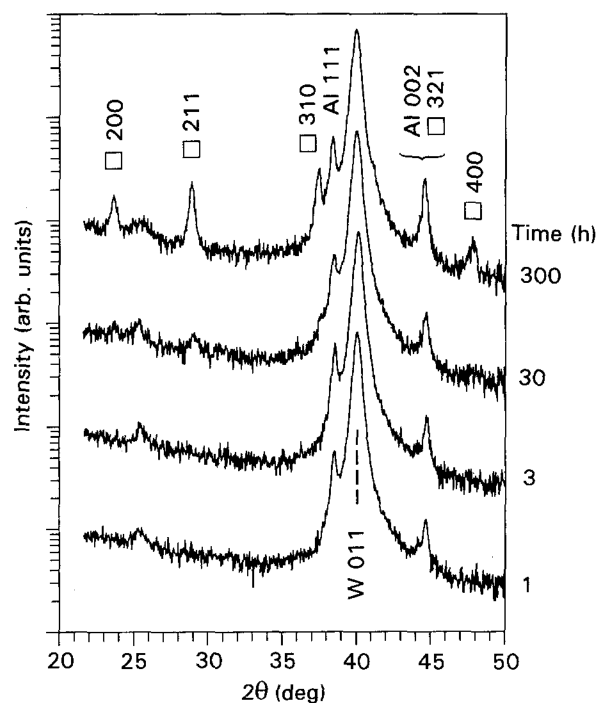

Figure 1 Thin-film X-ray diffraction patterns of films annealed at 400 °C. □, $Al_{12}W$.

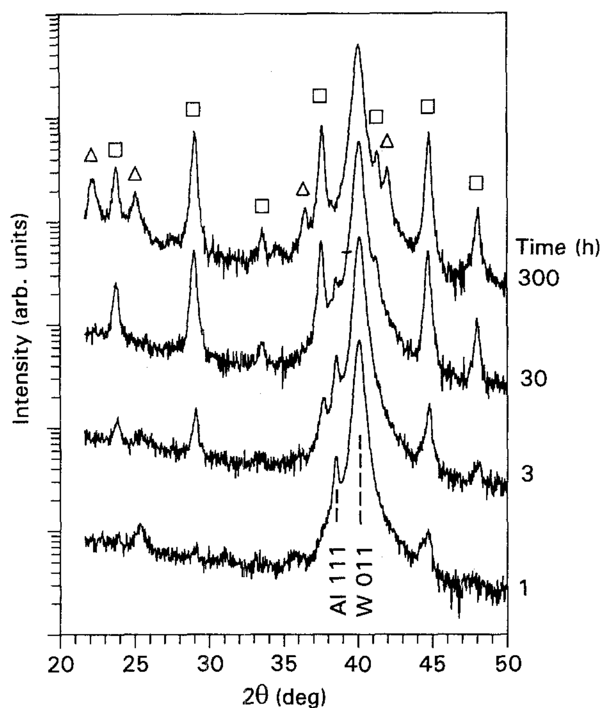

Figure 2 Thin-film X-ray diffraction patterns of films annealed at 450 °C. □, $Al_{12}W$; △, Al_4W.

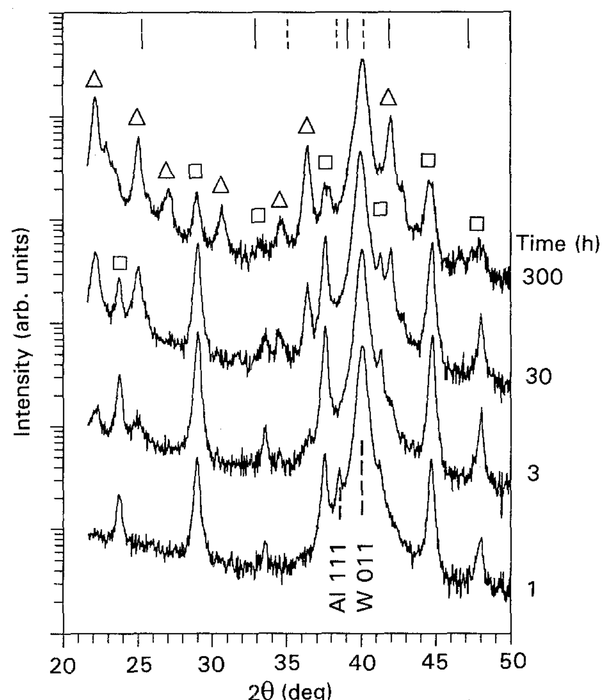

Figure 3 Thin-film X-ray diffraction patterns of films annealed at 500 °C. Standard peak positions, vertical lines (——) Al_3Ti; (– – –) Ti. □, $Al_{12}W$; △, Al_4W.

reflection of the body-centred-cubic phase of $Al_{12}W$. In the 300-h pattern, the $Al_{12}W$ (2 1 1) peak became stronger and in the meantime other $Al_{12}W$ peaks also began to appear. However, strong Al and W peaks are still present in the 300-h pattern indicating that although the Al/W interaction is well under way in this sample, there are still Al and W layers left unreacted.

The thin-film interaction at 450 °C is also dominated by $Al_{12}W$ formation for a reaction time of upto 30 h. This is borne out by the fact that the peaks in the 1-, 3- and 30-h spectra in Fig. 2 can all be ascribed to either W, Al or $Al_{12}W$. As expected, the $Al_{12}W$ peaks intensified while the Al (1 1 1) peak at $2\theta = 38.6°$ weakened with increasing reaction time. The Al (1 1 1) peak disappeared completely, with a concomitant development of several new peaks in the 300-h spectrum in Fig. 2. These new peaks can all be attributed to the monoclinic phase of Al_4W ($a = 0.5272$, $b = 17.771$, $c = 0.5218$ nm; $\beta = 100.2°$) [17]. According to the Al–W binary phase diagram [18], three intermetallic compounds exist in this system, $Al_{12}W$, Al_5W and Al_4W. It has been reported by several groups [8–10] that when the Al:TiW ratio is small, Al would be completely reacted with W to form $Al_{12}W$ first, and a prolonged interaction would lead to the formation of Al_5W and/or Al_4W.

The reaction proceeds much faster at 500 °C. The 1-h reaction at this temperature results in a fair amount of $Al_{12}W$ formation. Some Al still remains, however, as evidenced by the $Al_{12}W$ peaks and the Al small (1 1 1) peak in the 1-h spectrum in Fig. 3. After a 3-h reaction, the Al (1 1 1) peak disappeared completely while the $Al_{12}W$ peaks became stronger and several Al_4W peaks also showed up. In the 30- and 300-h spectra, we see a gradual increase in the intensity of Al_4W peaks with increasing reaction time, and a concomitant decrease in the intensity of $Al_{12}W$ peaks. This indicates that Al_4W forms at the expense of the $Al_{12}W$.

Our previous TEM results [9] have demonstrated the formation of Al_3Ti precipitates in the Al/TiW/SiO_2/Si system, but we were unable to detect the presence of Al_3Ti by thin-film XRD because of its small amount. Dirk *et al.* [12] recently also reported, that Ti_2W_8 film will be separated into W and Ti two phases after annealing (based on electron diffraction data). As both the precipitation of Al_3Ti and the separation of W and Ti in TiW are thermally activated processes, the high-temperature, long reaction time employed in this investigation should favour their occurrence. For this reason we have paid special attention to the 500 °C, 300 h sample in the hope of detecting W and Ti in the XRD pattern. However, the analysis of multiphase thin-film X-ray data is often difficult because diffraction peaks from different phases are frequently overlapped. Any identification based on one or two peaks should be viewed with extra caution. The standard powder diffraction data of hexagonal Al_3Ti and hexagonal Ti, taken from the JCPDS [19] #26–39 and #5–682 are listed in Table I (for brevity, only the reflections close to the 2θ range shown in Fig. 3 are listed). Columns 1 to 4 in this table show, respectively, the Miller index of the reflecting plane, *d*-spacing, relative intensity and the corresponding 2θ angle for the $CuK_{\alpha 1}$ radiation. Out of the five standard Al_3Ti reflections shown in Fig. 3, only two ($2\theta = 25.3°$ and $2\theta = 41.9°$) have matching experimental peaks. These two peaks, however, can be also ascribed to Al_4W (0 5 0) and Al_4W (2 1 1, 1 0 2), respectively. It is unlikely that these two peaks are from the Al_3Ti phase for the following reasons. (i) Table I shows that the two strongest peaks for Al_3Ti occur at

TABLE I Standard powder diffraction data for Al_3Ti and Ti.

hkl	d (nm)	I/I_{max}(%)	2θ
Al_3Ti (JCPDS #26-39)			
101	0.3520	40	25.3
110	0.2723	20	32.9
112,103	0.2303	100	39.1
004	0.2153	100	41.9
200	0.1926	80	47.2
Ti (JCPDS #5-682)			
010	0.2557	30	35.1
002	0.2342	20	38.4
011	0.2244	100	40.2
012	0.1726	19	53.0
110	0.1475	16	63.0

$2\theta = 39.1°$ and $2\theta = 41.9°$ with equal intensity. The 300-h spectrum in Fig. 3, however, only has one strong peak at 41.9°, while the 39.1° peak is completely missing. Also, the third strongest peak for Al_3Ti which should occur at 47.2° with a relative intensity of 80% is also missing. Therefore, the data are inconsistent with what is expected of randomly oriented Al_3Ti precipitates. (ii) The relative intensity for the 25.3° peak should be 40% of that for the 39.1° peak according to Table I, but the experimental data indicate a stronger peak at 25.3°. (iii) The preferred orientation of Al_3Ti precipitates may be invoked to explain the missing of some of the reflections, but this is considered unlikely because of the matrix ($Al_{12}W$ or Al_4W) in which Al_3Ti phase forms do not show the preferred orientation. (iv) The two peaks at 39.1° and 41.9° have comparable intensities relative to other Al_4W peaks and can be consistently assigned to the Al_4W phase.

If TiW alloy is decomposed into W and Ti after annealing, three peaks are expected for the Ti phase in the angular range shown in Fig. 3, (dashed lines). The strongest reflection for the Ti phase is (0 0 1) occuring at 40.2°. This peak, unfortunately, is overlapping the strongest W (0 1 1) peak, making it ambiguous for the identification of Ti. We therefore resort to the other two weaker reflections, one at 35.1° and the other at 38.4°, in the search of Ti phase. But Fig. 3 clearly shows that there is no peak at these two angular positions, implying that the Ti phase, if it exists, is below the detection limit of the XRD. Tungsten has only one peak located in the 20° to 50° range shown in Fig. 3, which is marked as W (0 1 1) at 40.3°. Other tungsten peaks outside this range were all observed with the correct relative intensities, as predicted by the standard pattern (JCPDS #4-806). The preceding detailed analyses of the X-ray results do not completely rule out the presence of Al_3Ti and Ti phases in our samples, but show that Al_3Ti and Ti are, at most, minor phases and will not be further considered in our kinetic analysis.

Figs 4–6 show cross-sectional TEM micrographs of the samples annealed at 400, 450 and 500 °C, respectively. The identification of each layer shown in these figures was determined by electron diffraction. It can be seen from Fig. 4 that the interaction between Al and W–Ti was weak at 400 °C. A continuous $Al_{12}W$ film formed only after reaction for 30 h or longer. However, traces of $Al_{12}W$ could be detected at the Al/W–Ti interface, even after a short reaction time at 400 °C, as evidenced by the arrows in the 1-h (Fig. 4a) and 3-h (Fig. 4b) samples. At 450 °C (see Fig. 5) a continuous layer of $Al_{12}W$ formed after a 1-h reaction and the thickness of this layer increased with increasing reaction time. Our previous study [9] on the isochronous reaction behaviour between Al and W–Ti had shown that a 55-nm-thick continuous $Al_{12}W$ film formed even after a much shorter 30-min anneal at 450 °C. The Al film disappeared completely and a monoclinic phase of Al_4W appeared at the $Al_{12}W$/W–Ti interface after 300 h at 450 °C (see Fig. 5d). The interaction of Al and W–Ti progressed rapidly at 500 °C. It is evident from Fig. 6a that over one half of the Al film had been consumed after 1 h at 500 °C. After 3 h (see Fig. 6b), only fragments of Al patches remained at the very top of the multilayer structure. Aluminium film no longer existed after 30 h; instead, a 260-nm-thick Al_4W layer formed between the top layer and the remaining W–Ti layer as shown in Fig. 6c. This continuous layer of Al_4W is highly

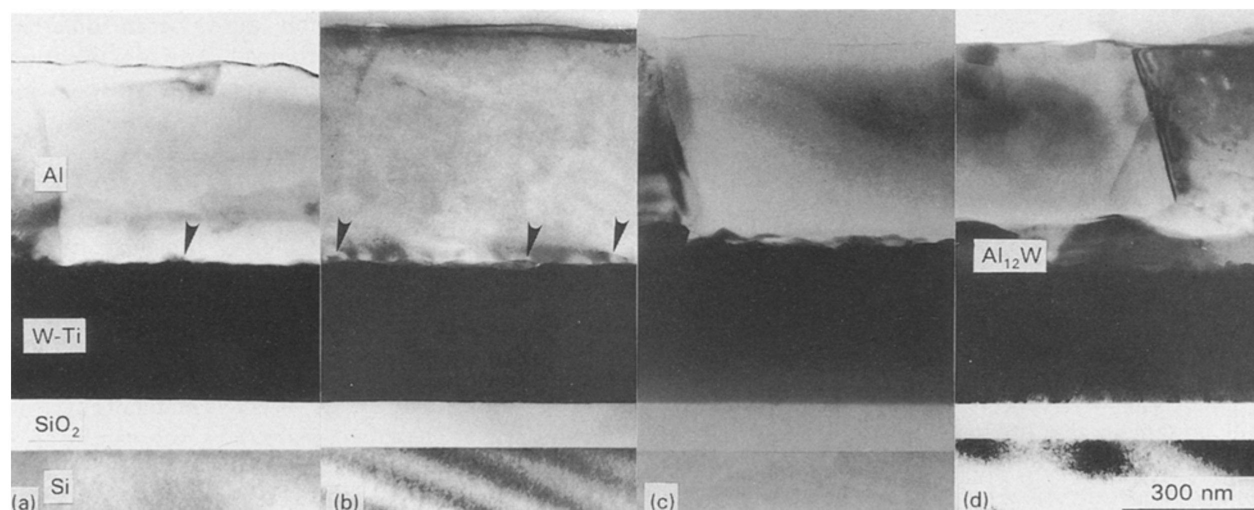

Figure 4 Cross-sectional TEM micrographs showing the structures of films annealed at 400 °C for (a) 1; (b) 3; (c) 30; (d) 300 h.

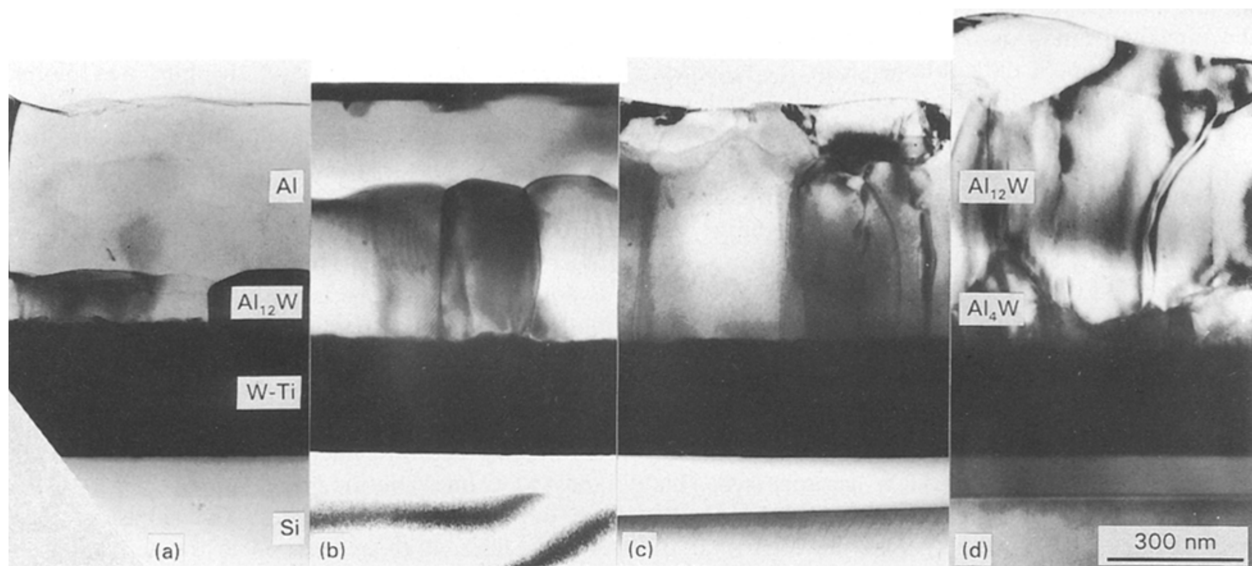

Figure 5 Cross-sectional TEM micrographs showing the structures of films annealed at 450 °C for (a) 1; (b) 3; (c) 30; (d) 300 h.

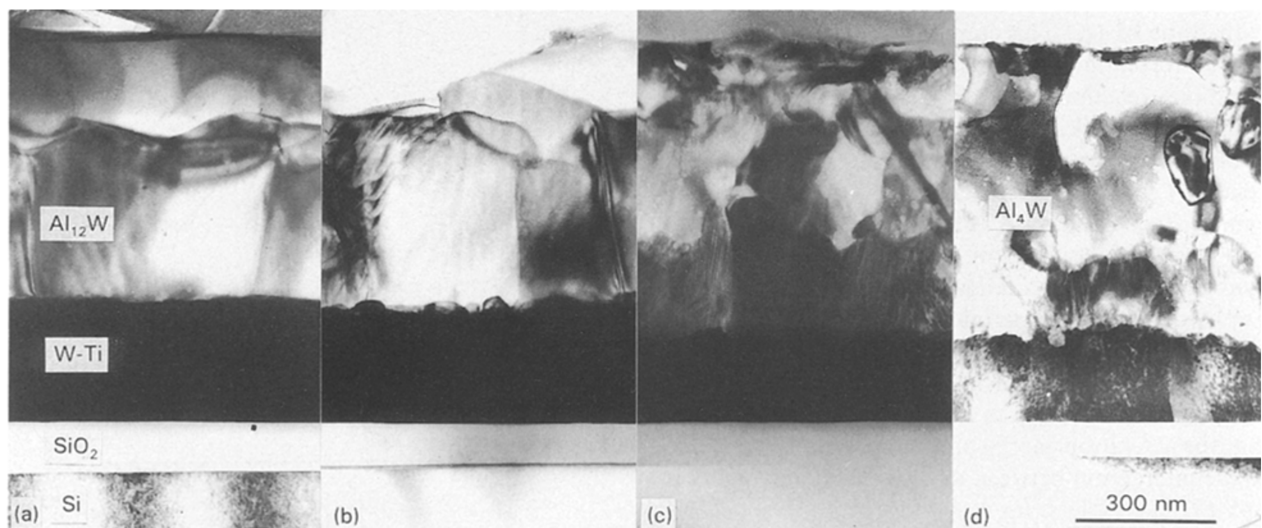

Figure 6 Cross-sectional TEM micrographs showing the structures of films annealed at 500 °C for (a) 1; (b) 3; (c) 30; (d) 300 h.

defective, with numerous microtwins. Detailed electron diffraction work on the Al_4W grain structures has been reported elsewhere [10]. The layer on top of the continuous Al_4W layer consisted primarily of a mixture of $Al_{12}W$ and Al_4W grains with a small quantity of Al_3Ti grains dispersed in it. After extended reaction (300 h) at 500 °C (see Fig. 6d), the continuous Al_4W layer thickness changed little, but the amount of Al_4W in the top mixed layer increased with a concomitant decrease in $Al_{12}W$ content. This explains the decrease in intensity of $Al_{12}W$ peaks and increase in intensity of Al_4W peaks, as discussed previously for the XRD data of this sample shown in Fig. 3.

The advantage of TEM in the study of thin-film interactions is its capability to measure directly the thickness of various layers in the specimens, allowing direct deduction of kinetic information. Table II summarizes the thickness data of various layers from all the specimens. In principle, if one knows the initial thickness of Al and W–Ti, the reacted Al and W–Ti can be calculated and reaction kinetics deduced therefrom. However, due to the inhomogeneity of the sputter-deposition process, the initial Al and W–Ti layer thicknesses vary within the same wafer by at least 10% and the variation is even worse across the wafers. These variations make the determination of the reacted Al and W layer thicknesses very uncertain. Also,

TABLE II Film thickness data.

Annealing		Layer thickness (nm)				
Temperature (°C)	Time (h)	SiO_2	TiW	Al	$Al_{12}W$	Al_4W
400	1	99	285	438	Trace	0
	3	89	283	504	8	0
	30	99	314	440.5	25	0
	300	81	283.5	395	95	0
450	1	92	287	397	97.5	0
	3	81	254	207	351	0
	30	117	251	107	438	0
	300	91	198	0	615	83
500	1	101	258	219	355	0
	3	97.5	231	Trace	443	33
	30	91	182	0	0	260
	300	69	178.5	0	0	260

we know that two compound reactions occur under the annealing conditions studied in this investigation, therefore any kinetic data obtained from the thickness change of Al or W–Ti layers will be the combined result of $Al_{12}W$ and Al_4W reactions. For the above reasons we will not attempt to extract kinetic data from the thickness data of Al and W–Ti directly.

It is possible to obtain kinetic data for the $Al_{12}W$ reaction directly from its thickness data. However, caution should be exercised in using the $Al_{12}W$ thickness data in Table II because $Al_{12}W$ was involved in two competing reactions: (i) $Al_{12}W$ formation due to the Al/W–Ti interaction; and (ii) $Al_{12}W$ consumption due to the $Al_{12}W$/W–Ti interaction. For the study of $Al_{12}W$ formation, thickness data should be excluded from the specimens in which Al_4W has appeared. This is done in Fig. 7 where the logarithm of the $Al_{12}W$ layer thickness is plotted against the logarithm of reaction time at 400 and 450 °C (the 500 °C data were not analysed because the Al_4W reaction sets in very early at this temperature). The data for each temperature in Fig. 7 can be fitted by parallel straight lines with slope of 1/2. This implies that the $Al_{12}W$ compound formation is diffusion-controlled, obeying a parabolic reaction law: $y = A(T)\ t^{\frac{1}{2}}$, where y is the $Al_{12}W$ layer thickness, t is reaction time, and $A(T)$ is a temperature-dependent reaction-rate constant. $A(T)$ generally follows an Arrhenius equation: $A(T) = A_0 \exp(-Q/kT)$, where A_0 is a constant, Q is the activation energy of the reaction, and k and T are Boltzman constant and reaction temperature, respectively. $A(T)$ can be determined experimentally from the intercepts of the lines with the y axis in Fig. 7. The activation energy can be obtained from the slope of a plot of $A(T)$ against $\log(1/T)$, as in Fig. 8. This figure shows that the activation energy of the $Al_{12}W$ formation due to the interaction between Al–1 wt % Si and W–Ti is 2.45 eV.

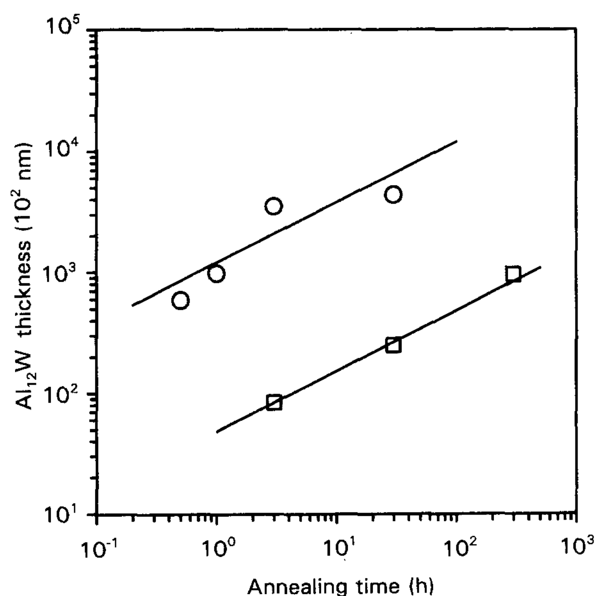

Figure 7 The variation of $Al_{12}W$ layer thickness as a function of reaction time at two temperatures (450 °C, 0.5 h data from [9]). ○, 450; □, 400 °C.

The activation energy for the $Al_{12}W$ formation can also be determined from the sheet-resistance data. In Fig. 9 the sheet resistance of the film was plotted against the square root of reaction time for the three temperatures studied. Generally, the change in sheet resistance can be attributed to the compound reactions, and a linear relationship in this kind of plot reflects a diffusion-controlled reaction mechanism. Microstructurally, it has been shown that the reaction is dominated by $Al_{12}W$ formation at 400 and 450 °C, but two reactions occur at 500 °C. This is also borne out in Fig. 9, where the 400 and 450 °C data are linear, but the 500 °C data can be fitted with two straight lines with different slopes. It is reasonable, based on the microstructural evidence, to assume that the 400 and 450 °C lines and the initial part of the 500 °C line are due to $Al_{12}W$ formation. The slopes of these straight lines, $B(T)$, are related to the activation en-

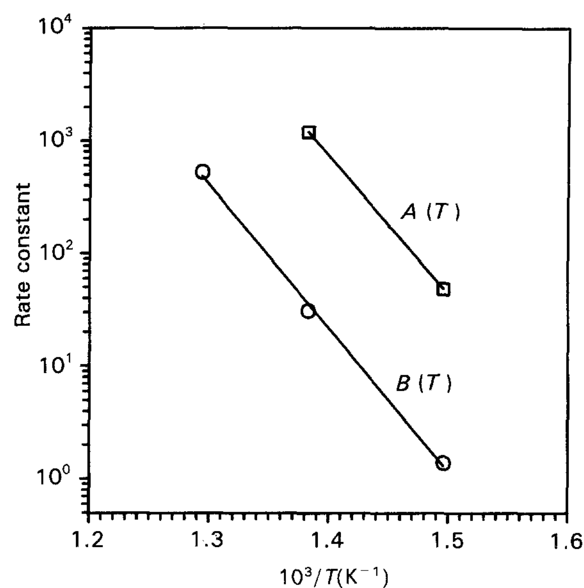

Figure 8 Temperature dependence of the rate constant for $Al_{12}W$ formation. □, Thickness; ○, resistance.

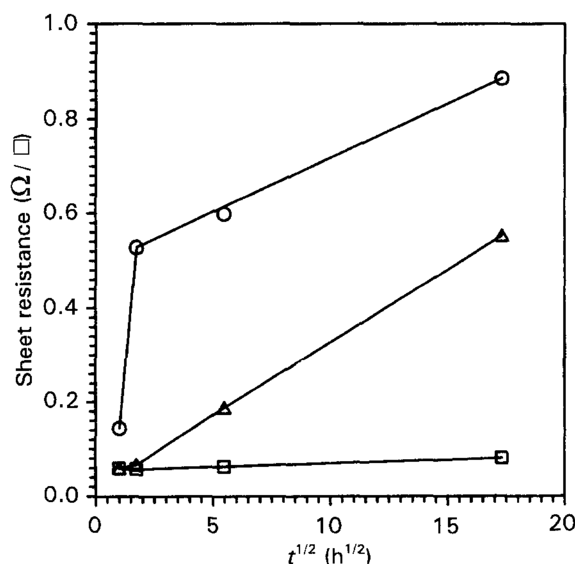

Figure 9 Sheet resistance as a function of reaction time at three temperatures. ○, 500; △, 450; □, 400 °C.

ergy of compound formation in an Arrhenius equation $B(T) = B_0 \exp(-Q/kT)$. In Fig. 8, log $[B(T)]$ is plotted against $\log(1/T)$ and the activation energy determined from the slope is 2.53 eV, which is in excellent agreement with the value of 2.45 eV obtained from the thickness data. The value of 2.53 eV probably is more reliable than 2.45 eV for the $Al_{12}W$ reaction, because the measurement of the sheet resistance is more accurate than the thickness measurement, and also because three data points were used in the determination of activation energy in the case of sheet resistance, while only two were used in the case of the thickness data in Fig. 8. Colgan [11] has recently reviewed the data on thin-film aluminide formation; the typical activation energy of the transitional metal aluminide varies from 1.5 eV for $HfAl_3$, $NiAl_3$ and $NbAl_3$ to 2.7 eV for VAl_3 and $CrAl_7$. An extremely large activation energy of 4.9 eV has been reported for $MoAl_{12}$ [20]. Relative to other transition-metal aluminides, the activation energy of $Al_{12}W$ is apparently on the higher end.

With the aid of the TEM microstructural data shown previously, it can also be concluded from Fig. 9 that the sheet resistance of Al/W–Ti film does not change significantly as long as a continuous Al film still exists in the system. The Al film is completely converted to $Al_{12}W$ after 450 °C for 300 h or 500 °C for 3 h (there is a very thin layer of Al_4W present at the $Al_{12}W$/W–Ti interface in these two samples, but its effect on sheet resistance is negligible). The sheet resistances for these two samples are very similar and can be attributed to the $Al_{12}W$ phase alone. Therefore it may be inferred that the sheet resistance of $Al_{12}W$ film is about 570 m$\Omega/\square$.

The data obtained on the Al_4W compound formation are insufficient to warrant any kinetic analysis. The Al_4W reaction is quite different from the $Al_{12}W$ reaction, in that a continuous layer forms initially as a result of interaction between $Al_{12}W$ and W–Ti, but its thickness remains essentially constant at about 260 nm. A longer reaction time does not affect the continuous Al_4W layer thickness, but only converts the $Al_{12}W + Al_4W$ mixed layer (which is on top of the continuous Al_4W layer) to a higher Al_4W content. This indicates that the reaction kinetics for Al_4W formation are very sluggish, and the reaction slows down as more Al_4W is formed. Further studies are needed to understand the kinetics of the Al_4W reaction in detail.

4. Conclusion

Thin-film interactions between Al–1 wt % Si and W–Ti barrier layers in the $Al/Ti_3W_7/SiO_2/Si$ system are diffusion controlled. A body-centred-cubic phase of $Al_{12}W$ forms firstly at the Al/W interface. A monoclinic phase of Al_4W forms at the $Al_{12}W$/W–Ti interface when Al film is about to be completely consumed. Al_3Ti is a minor phase formed as precipitates in $Al_{12}W$ matrix, and the decomposition of TiW alloy into W and Ti is below the detection limit of thin-film XRD. The activation energy of $Al_{12}W$ compound formation, due to the interaction between Al–1% Si and W–Ti, is 2.45 eV as determined from the thickness data, and 2.53 eV as determined from the sheet resistance data. The sheet resistance of the film is relatively constant if Al remains a continuous film, but increases dramatically if the reaction proceeds such that Al film is no longer continuous. The sheet resistance of the $Al_{12}W$ film is estimated to be 570 m$\Omega/\square$.

Acknowledgement

This work was partially supported by the National Science Council, Republic of China, under the contract number NSC 79-0404-E-009-49.

References

1. R. ROSENBERG, M. J. SULLIVAN and J. K. HAWARD, in "Thin Films-Interactions and Reactions", edited by J. M. Poate, K. N. Tu and J. W. Mayer (Wiley, New York, 1978) p. 13.
2. P. B. GHATE, *Physics Today* **39** (1986) 58.
3. J. O. OLOWOLAFE, C. J. PALMSTROM, E. G. COLGAN and J. W. MAYER, *J. Appl. Phys.* **58** (1985) 3440.
4. S. BERGER, Y. KOMEM and I. BLECH, *Thin Solid Films* **176** (1989) 131.
5. S. BERGER, Y. KOMEM and B. Z. WEISS, *J. Appl. Phys.* **69** (1991) 4341.
6. P. B. GHATE, J. C. BLAIR, C. R. FULLER and G. E. MCGUIRE, *Thin Solid Films* **53** (1978) 117.
7. C. Y. TING and M. WITTMER, *ibid.* **96** (1982) 327.
8. C. J. PALMSTROM, J. W. MAYER, B. CUNNINGHAM, D. R. CAMPBELL and P. A. TOTTA, *J. Appl. Phys.* **58** (1985) 3444.
9. P.-H. CHANG, H.-Y. LIU, J. A. KEENAN, J. M. ANTONY and J. G. BOHLMAN, *J. Appl. Phys.* **62** (1987) 2485.
10. P.-H. CHANG, H.-M. CHEN and H.-Y. LIU, *ibid.* **72** (1992) 2739.
11. E. G. COLGAN, *Mater. Sci. Rep.* **5** (1990) 1.
12. A. G. DIRK, R. A. M. WOLTERS and A. J. M. NELLISSEN, *Thin Solid Films* **193/194** (1990) 201.
13. S. E. BABCOCK and K. N. TU, *J. Appl. Phys.* **53** (1982) 6898.
14. I. KRADCSIK, J. GYULAI, C. J. PALMSTROM and J. W. MAYER, *Appl. Phys. Lett.* **43** (1983) 1015.
15. H.-Y. LIU, P.-H. CHANG, J. G. BOHLMAN and H.-L. TSAI, *Mater. Res. Soc. Symp. Proc.* **119** (1988) 153.
16. P.-H. CHANG, M. D. COVIELLO and A. F. SCOTT, *ibid.* **115** (1988) 93.
17. J. A. BLAND and D. CLARK, *Acta Cryst.* **11** (1958) 231.
18. T. B. MASSALSKI, T. B. OKAMOTO, P. R. SUBRAMANIUM and L. KACPRZAK, "Binary Alloy Phase Diagrams", 2nd edn (ASM International, Ohio, 1990) p. 235.
19. JCPDS 19081 (Joint Committee on Powder Diffraction Standards, 1601 Park Lane, Swarthmore, Pennsylvania, USA).
20. R. N. SINGH, D. M. BROWN, M. J. KIM and G. A. SMITH, *J. Appl. Phys.* **58** (1985) 4598.

Received 2 April
and accepted 19 October 1993